Carbohydrate Polymers 97 (2013) 618–626

Contents lists available at SciVerse ScienceDirect

Carbohydrate Polymers

journal homepage: www.elsevier.com/locate/carbpol

Osteoblast differentiation and phenotype expressions on chitosan-coated Ti-6Al-4V

Hsin-Yi Lin [a,*], Jing-Huei Chen [b]

[a] Department of Chemical Engineering and Biotechnology, National Taipei University of Technology, 1, Section 3, Zhongxiao E. Road, Taipei 106, Taiwan
[b] Graduate Institute of Biotechnology, National Taipei University of Technology, 1, Section 3, Zhongxiao E. Road, Taipei 106, Taiwan

ARTICLE INFO

Article history:
Received 22 December 2012
Received in revised form 25 April 2013
Accepted 20 May 2013
Available online 27 May 2013

Keywords:
Surface modification
Chitosan
Pectin
Alginate
Titanium implant
Bone repair

ABSTRACT

Chitosan (C), alginate-crosslinked chitosan (CA), and pectin-crosslinked chitosan (CP) were covalently bonded to Ti-6Al-4V surfaces and tested for their biocompatibility. Compared to the clinically treated Ti-6Al-4V surface (Ti64), C, CA, and CP, had higher contact angles and promoted higher cell proliferation, type I collagen deposition, and mineralization after two weeks (all $p < 0.05$). Cells on C, CA, and CP expressed more alkaline phosphatase (ALP) activity compared to those on Ti64 ($p < 0.05$). The swelling ratios and drug release efficacies of CA and CP were significantly higher and lower, respectively, than those of C (both $p < 0.05$). Only cells on CA expressed ALP activity after three weeks of culture. Generally speaking, crosslinking with alginate and pectin changed surface wettability as well as the swelling and drug release properties of the chitosan coatings. Cells on the coatings had higher proliferation, type I collagen deposition, and degree of mineralization compared to those on Ti64.

1. Introduction

Osteointegration is essential for the successful implantation of an orthopedic prosthesis in a human body. Ti-6Al-4V titanium alloy is one of the most commonly used orthopedic materials because of its high mechanical strength, durability, corrosion resistance, and biocompatibility (Head, Bauk, & Emerson, 1995). Surface modifications have been investigated to improve the clinical performances of titanium and its alloys. Researchers have attempted coating Ti and its alloys with collagen (Becker et al., 2002; Bierbaum et al., 2003; Geissler et al., 2000), chitosan (Bumgardner, Wiser, & Elder, et al., 2003; Bumgardner, Wiser, & Gerard, et al., 2003; Greene, Bumgardner, Yang, Moseley, & Haggard, 2008), hydroxylapatite (Aksakal & Hanyaloglu, 2008), and calcium phosphate (Cleries, Fernandez-Pradas, & Morenza, 2000) to improve their cell adhesion, proliferation, and differentiation performances and also to carry desirable compounds on their surfaces.

Chitosan has been reported to enhance bone and cartilage tissue formation because the molecular structure of chitosan is similar to the components of the extracellular matrix of bone cells (Abarrategi et al., 2010; Schwartz, Griffon, Fredericks, Lee, & Weng, 2011). Chitosan, coated on pure titanium surfaces through silane bonding, has been reported to be stable for weeks and to promote serum protein adsorption and the growth of osteosarcoma cells (Bumgardner, Wiser, & Elder, et al., 2003; Bumgardner, Wiser, & Gerard, et al., 2003). Chitosan hydrogels have been crosslinked using natural polymers such as alginate and pectin to further improve their biocompatibility and mechanical properties (Lin & Yeh, 2010a, 2010b). Alginate is a brown seaweed extract that has been shown to elicit little or no immune reaction in nearby tissues (Klock et al., 1997; Tang, Chen, Weir, Thein-Han, & Xu, 2012). *In vitro* and *in vivo* results have shown that alginate is osteogenic (Lin & Yeh, 2010a; Tang et al., 2012; Xing et al., 2013; Yang, Frei, Rossi, & Burt, 2009). Pectin is contained in the primary cell walls of terrestrial plants and is a natural crosslinker of chitosan (Kim, Park, Kim, & Cho, 2003; Li et al., 2011). *In vitro* results have shown that pectin has good biocompatibility and is osteogenic (Kokkonen et al., 2008, 2010, 2012; Lin & Yeh, 2010b). Pectin and alginate are both anionic polysaccharides, which crosslink with chitosan, a cationic polysaccharide, through ionic attraction between the NH_3^+ of chitosan and the COO^- of alginate and pectin.

To the authors' best knowledge, the biocompatibility of Ti-6Al-4V surface modified with alginate- and pectin-crosslinked chitosan has not been investigated. In this study, chitosan was covalently coated on Ti-6Al-4V through silanization and further crosslinked with alginate and pectin. The changes in physical and biological properties after crosslinking were measured and compared to those of the chitosan coating and the Ti-6Al-4V surface used for implants. The physical properties of the coatings that were

* Corresponding author. Tel.: +886 2 27712171x2546; fax: +886 2 27317117.
E-mail addresses: hbrunken@ntut.edu.tw, hsin_yi_lin@yahoo.com (H.-Y. Lin), jinghueigrandma@hotmail.com (J.-H. Chen).

0144-8617/$ – see front matter © 2013 Elsevier Ltd. All rights reserved.
http://dx.doi.org/10.1016/j.carbpol.2013.05.048

measured included their thickness, wettability, swelling ratio, and drug release efficacy. Mature osteoblasts were cultured on the Ti-6Al-4V surface and the coatings for three weeks. The biological responses of osteoblast cells – including cell proliferation, viability, morphology, type I collagen expression, alkaline phosphatase activity, and mineralization – were assayed.

2. Materials and methods

All chemicals were purchased from ACROS (NJ, USA) unless otherwise specified.

2.1. Coating the polymer on the titanium alloy surface

Medical grade Ti-6Al-4V ELI (ASTM F136) was purchased from Titanium Industries Asia Inc. – Taiwan Branch (Taipei, Taiwan). The alloy was cut into two sizes (1 cm × 1 cm × 1 mm and 5 cm × 5 cm × 1 mm) to be used in different tests. The surfaces of the Ti-6Al-4V plates were treated as described by (Bumgardner, Wiser, & Gerard, et al., 2003) before being coated with chitosan. Briefly, the plates were submerged in a 95% (v/v) ethanol solution (pH 4.5) and 2% (v/v) of 3-isocyanatopropyltriethoxysilane was added to the solution. The pH was maintained at 4.5–5.5 with 1 M NaOH or 10 M acetic acid. Ten minutes later the plates were rinsed with ethanol and heated at 110 °C for 10 min. The plates then were submerged in a 2% (v/v) glutaraldehyde solution at pH 4.3 overnight. The plates were rinsed with de-ionized water. Chitosan (96% deacetylation, M.W. = 300 kDa, Charming & Beauty, Taiwan) was dissolved in 1% acetic acid to make a 2% (w/v) chitosan solution. For the 1 cm^2 and 25 cm^2 plates, 200 μL and 4 mL, respectively, of the chitosan solution was homogeneously spread on the treated Ti-6Al-4V surface and dried at 40 °C in an oven for 8 hr. The dry coatings were neutralized in 10 N NaOH for 5 min and washed in deionized water. Sodium alginate and pectin (~70% methoxylation) were dissolved in deionized water to make 2% (w/v) solutions. These two solutions were used to crosslink the coated chitosan with 200 μL and 4 mL crosslinkers for the 1 cm^2 and 25 cm^2 chitosan coatings respectively. The crosslinker was homogeneously spread across the top of the chitosan coating. One hour later, the coatings were washed three times in deionized water to remove the unbound crosslinker. The alginate solution on the chitosan coating was hard to be completely removed by simple rinsing due to its high viscosity. Hence the alginate-crosslinked chitosan was submerged in 10% (w/v) $CaCl_2$ solution overnight, while the other coatings were kept in deionized water. The alginate-coated chitosan was rinsed several times with water to remove $CaCl_2$ and the debris of the residual alginate from the coating. The chitosan coated Ti-6Al-4V plates will be referred to as C, alginate-crosslinked chitosan coating as CA, and pectin-crosslinked chitosan coating as CP. The Ti-6Al-4V surfaces that were prepared following the guidelines in ASTM F86-12: *Standard Procedure for Surface Preparation and Marking of Metallic Surgical Implants* were used as positive control and referred to as Ti64. The control plates were wet ground with 80 grit SiC paper and ultrasonically cleaned for 10 min each in de-ionized water, ethanol, acetone, and ethanol again. They were passivated in 30% nitric acid for 30 min and rinsed in de-ionized water.

2.2. Peeling strength, thickness of the coating and contact angle measurements

The peeling test was performed on all three coatings to verify whether the bonding strength between the coatings and the metal surface changed after crosslinking. ASTM D903-98(2010) *Standard Test Method for Peel or Stripping Strength of Adhesive Bonds* was used for this test. The coating was partially peeled, and then its free end was folded back to a 180° angle. There was approximately 2 cm of separation between the free end of the coating and the metal. The metal surface was secured with a Vice-Grip on the crosshead of a tensile tester (Kotsao, Taiwan) while the free end of the coating was secured with using another Vice-Grip. The crosshead moved upward at a rate of 6 mm/min until the coating had almost peeled off the metal. Data from the coatings torn during the test were not used to calculate the results. Load (N) vs. peeling distance (mm) was then plotted, and the data points after the load reached a plateau were averaged and used as the peeling strength of the particular sample. The peeling strengths from six successful tests were averaged for each coating ($n = 6$).

The thickness of the coating was measured using a Surface Roughness Tester (Mahr S2, Mahr GmbH, Göttingen, Germany) ($n = 6$). Only half of the metal sample was coated with polymer while the other half was left uncoated. The probe of the Tester moved against the surface from the uncoated side to the polymer-coated side. The change in the probe's altitude was used to determine the thickness of the coating. The contact angle was then measured ($n = 4$) to assess the wettability of the surfaces. Deionized water (5 μL) was placed on the coating, and the contact angle was recorded using a FACE Contact Angle Meter (Kyowa Interface Science, Japan).

2.3. Swelling ratio

Dry 1 cm × 1 cm coated sample plates were weighed, and their weights were recorded (W_0) ($n = 5$). They were placed in a beaker filled with 100 mL of phosphate buffered saline (PBS, pH = 7.4). At different sampling times for up to 60 min, the plates were taken out of the beaker. The excess water on the plates was removed by gently tapping the plates on low-lint tissue (Kimwipes, Kimberly-Clark, WI) before their final weights were recorded (W_f). The polymer coating on each plate was carefully removed by a pair of tweezers, and the weight of the bare metal was measured (W_{Ti}). The swelling ratios of the coatings were calculated as $[(W_f - W_{Ti}) - (W_0 - W_{Ti})/(W_0 - W_{Ti})]$.

2.4. Drug release efficacy

The model drug used to test the release efficacies of the coatings was pentoxifylline (PTX, $C_{13}H_{18}N_4O_3$, Sigma, MO). PTX has been used clinically to reduce inflammation and fibroblast proliferation and subsequent fibrosis (Berman B, 1989).

Each coated sample (5 cm × 5 cm) ($n = 6$) was submerged in 7 mL of 2 mg/mL PTX solution and placed on a shaker (50 rpm). After 48 h, the absorbance of the solution was read at 274 nm (μQuant microplate reader, Biotech, USA), and the concentration of PTX, C_f (mg/mL), was determined using a standard curve. The amount of PTX loaded in each coating was W_L (mg) = 2 (mg/mL) × 7 (mL) − $C_f V_f$. The final volume of the PTX solution was V_f (mL). Each PTX-loaded sample was then placed in 10 mL PBS. At different sampling times, 100 μL of the PBS was removed, and the absorbance was read to calculate the amount of PTX in the solution at that time (W_t (mg)). The amount of PTX released was divided by the total amount of PTX loaded into the coating to obtain the release efficacy (W_t/W_L).

2.5. Cell culture

Osteoblast cells (7F2, CRL-12557, ATCC, VA) were cultured in α-MEM (Invitrogen, Carlsbad, CA), supplemented with 10% (v/v) fetal bovine serum + 100 IU/ml penicillin + 100 μg/ml streptomycin + 1 mM sodium pyruvate (all cell culture reagents were purchased from Invitrogen), and maintained in a CO_2 incubator (5% CO_2, 95% humidity, 37 °C; Astec, Fukuoka, Japan).

Samples (Ti64, C, CA, and CP; 1 cm × 1 cm) were submerged in 70% ethanol and rinsed with sterile PBS before being placed in 24-well tissue culture plates. Osteoblasts in osteogenic medium (α-MEM + 10% fetal bovine serum + 100 IU/ml penicillin + 100 μg/ml streptomycin + 1 mM sodium pyruvate + 50 μg/ml ascorbic acid + 10 mM β-glycerophosphate) were seeded on each sample at 10^4 cells/cm^2. The osteogenic culture medium was changed every other day. The following assessments on the cells were performed at 1, 2, and 3 weeks after cell seeding.

2.6. Proliferation

The cell proliferation was measured using a commercial cell counting kit (CCK-8, Sigma, MO, USA) following the manufacturer's directions. Briefly, 500 μL of fresh medium and 50 μL of 2-(2-methoxy-4-nitrophenyl)-3-(4-nitrophenyl)-5-(2,4-disulfophenyl) – 2H-tetrazolium monosodium salt (WST-8) were added to each sample. The samples were placed in a CO_2 incubator for 4 h. The culture medium absorbance was read at 450 nm.

2.7. Cell viability

Cell viability at the end of each test was qualitatively assessed using the Live/Dead® viability stain (Molecular Probe, OR) following the manufacturer's directions. Cells on the samples ($n = 3$) were washed with PBS and incubated with 100 μL LIVE/DEAD® reagent (2 mM Calcein AM + 4 mM ethidium homodimer-1) for 30 min at 37 °C. The cells were observed using a fluorescent microscope (CK X41, Olympus, Japan). Viable cells appeared green while dead cells appeared red.

2.8. Cell morphology

Cells on the 1 cm × 1 cm samples ($n = 4$) were crosslinked by 2.5% (v/v) glutaldehyde/PBS for 30 min. The samples were rinsed in deionized water, dehydrated in ethanol solutions (20%, 50%, 70% and 100%) and hexamethyldisilazane (Alfa Aesar, UK), and air dried. The cells were sputter-coated with Au–Pd using an Ion Sputter (E1010, Hitachi, Tokyo, Japan) and examined using a scanning electron microscope (SEM, S-3000H, Hitachi, Japan).

2.9. Alkaline phosphatase (ALP) activity

Each sample ($n = 4$) was placed in 500 μL of 0.1% Triton x-100 in 0.1 M of Tris buffer (pH = 7.2) and sonicated for 5 min. The cell lysate (50 μL) was incubated with a 200 μl substrate buffer (5 mM disodium p-nitrophenyl phosphate hexahydrate in 0.05 M 2-amino-2-methyl-1-propanol with 2 mM $MgCl_2$) at 30 °C for 60 min. ALP converted the substrate to p-nitrophenyl phosphate (p-NP). The absorbance of p-NP was read at 405 nm, and the enzyme activity was shown as the amount of p-NP (mM).

2.10. Type I collagen expression in the extracellular matrix

The amount of type I collagen secreted in the extracellular matrix was measured using a Sircol™ Collagen Assay (Biocolor, UK) in accordance with the manufacturer's instructions ($n = 4$). One milliliter of 0.5 M acetic acid with 0.1 mg/mL pepsin (Sigma, MO) was added to each sample and kept at 4 °C overnight. The acidic extract was moved to a microcentrifuge tube, and 100 μL Acid Neutralizing Reagent and 200 μL Isolation & Concentration Reagent were then added to it. The mixture was incubated overnight at 4 °C, and the tube was centrifuged at 12,000 rpm for 10 min. The supernatant was discarded, and 1 mL of Sircol Dye Reagent was added to the precipitation for 30 min before centrifugation. The supernatant was removed, and the pellet was rinsed with 750 μl Acid-Salt Wash Reagent followed by centrifugation. All the liquid was then removed, and Alkali Reagent (250 μl) was added to the tube before the absorbance of the liquid was read at 555 nm. The absorbance was converted to concentration (mg/mL) using a standard curve.

Table 1
Peeling strength (N), coating thickness (μm), and contact angle (degree) of the three polymer coatings and the clinically prepared Ti64 surface.

Coating	Peeling strength (N)	Coating thickness (μm)	Contact angle (degree)
Ti64[a]	n.a.	n.a.	63.5 ± 0.8[b]
C	0.715 ± 0.068[b]	34.4 ± 0.8	79.7 ± 1.5[c]
CA	0.852 ± 0.052[c]	33.0 ± 1.3	74.2 ± 2.1[d]
CP	1.060 ± 0.082[d]	32.9 ± 2.9	84.0 ± 2.4[e]

[a] Titanium surface prepared according to ASTM F86-12.
[b] Different letters indicate statistical significance ($p < 0.05$).
[c] Different letters indicate statistical significance ($p < 0.05$).
[d] Different letters indicate statistical significance ($p < 0.05$).
[e] Different letters indicate statistical significance ($p < 0.05$).

2.11. Calcium deposition in the extracellular matrix

Each sample ($n = 4$) was washed with PBS to remove the culture media and was submerged in 0.5 mL of 0.5 N acetic acid for 24 h at 37 °C. The acidic extract (10 μL) was mixed for 10 min with 300 μL of a working solution that contained 1.65 mM o-Cresolphthalein, 14.8 M ethanolamine/boric acid buffer, and 0.34 mM 8-hydroxyquinoline. The absorbance was read at 575 nm and converted into calcium concentration (μg/mL).

2.12. Von Kossa calcium stain

Cells on the samples ($n = 4$) were rinsed with PBS before being submerged in 10% formalin/PBS for 30 min. Formalin was discarded and 200 μL of 5% (w/v) silver nitrate solution was added to each sample. The samples were kept in complete darkness for 1 h before being rinsed with deionized water and exposed to UV light for 15 min. Pictures of the Ti64 were taken using a digital camera (Cannon A640 PowerShot, Japan). The polymer coatings were carefully removed from the Ti64 surfaces and examined under a light microscope (CKX41, Olympus, Japan).

2.13. Statistical analysis

Results are expressed as the mean ± standard deviation (SD) and compared by two-way analysis of variance (ANOVA) using the SigmaStat software package (Systat Software, Chicago, IL). When significant differences were found, pairwise comparisons were performed using Tukey's test. P values <0.05 were considered statistically significant.

3. Results and discussion

3.1. Peeling strength, thickness and contact angle of the coatings

The average loads used to peel C, CP, and CA off of the metal surface are listed in Table 1. Crosslinking with pectin and alginate both significantly increased the peeling strength of the coatings ($p < 0.05$), which indicates a stronger bond between the crosslinked coatings (CA, CP) and the metal surface than compared to C. Further experimentation is needed to explain the chemistry behind these changes in bonding strength. We speculate that the increase in bonding strength could be a result of more time spent submerged in an aqueous solution during the crosslinking process because it allowed more time for the chitosan molecules to react with

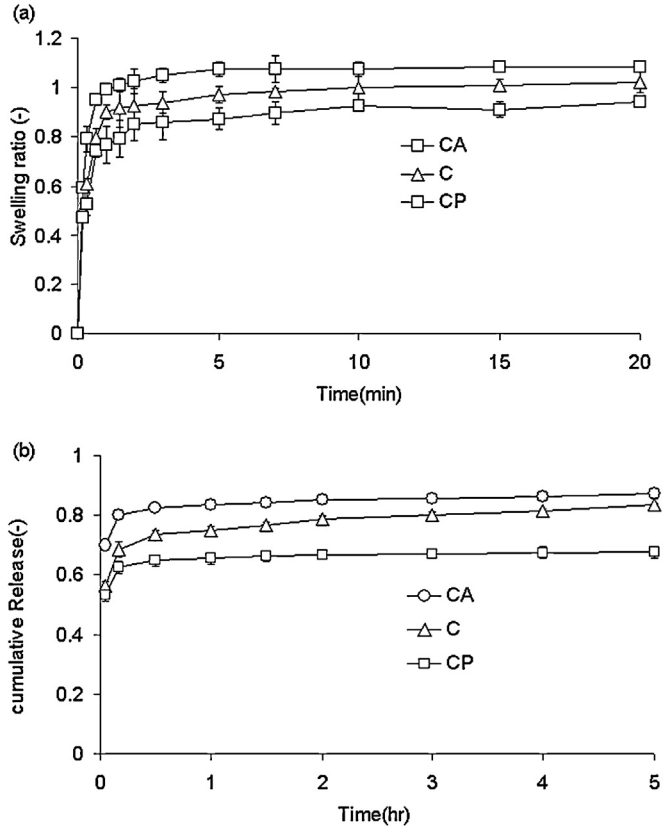

Fig. 1. Swelling ratio (a) and cumulative release of pentoxifylline (b) of C, CA, and CP.

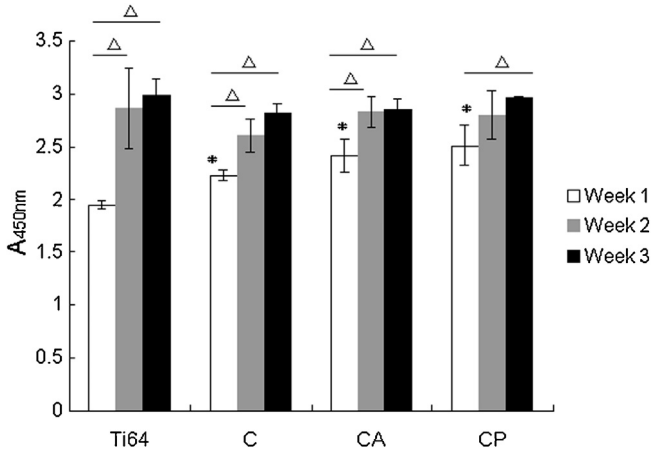

Fig. 2. Cell proliferation on Ti64, C, CA, and CP over three weeks. * and # indicate significant difference compared to Ti64 and C, respectively, measured at the same time ($p < 0.05$). △ and ○ indicate significant difference compared to week 1 and week 2, respectively, measured within the same material ($p < 0.05$).

the glutaraldehyde residues on the metal surface (Bumgardner, Wiser, & Gerard, et al., 2003). Regardless, all coatings tested were well attached to the metal surface during the course of all experiments.

The C, CA, and CP coatings had similar thicknesses of approximately 33 μm. The thicknesses of the coatings did not show a significant change after crosslinking ($p > 0.05$) (Table 1). CA had a smaller contact angle than C ($p < 0.05$) while CP had a larger one ($p < 0.05$). The contact angle of Ti64 (63.5°) was similar to what has been previously reported by Park et al. (2010) (58.1°), and the contact angle of C (79.7°, 96% deacetylated) was similar to what has been previously reported by Bumgardner, Wiser, and Elder, et al. (2003) (76.4°, 91.2 deacetylated). For CA, the OH and COO^- groups on the alginate molecules formed hydrogen bonds with water molecules, increasing its wettability compared to that of C. Pectin, with its high degree of methoxylation on the carboxyl groups, made CP less hydrophilic and wettable than C.

3.2. Swelling ratio

All coatings were saturated with water after less than 5 min in PBS (Fig. 1(a)). CA had the highest swelling of all ($p < 0.05$) because of it having the highest wettability. CP, being less wettable than C, had a lower swelling ratio compared to C ($p < 0.05$). Rapid saturation with water is advantageous for implant application. Once the water molecules and ions saturate the implant surfaces or coatings, serum proteins begin to deposit on the surfaces sequentially facilitating cell attachment and proliferation (Bumgardner, Wiser, & Elder, et al., 2003; Singhatanadgit, 2009).

3.3. Release efficacy of the anti-inflammatory drug PTX

The pattern of the PTX release efficacies of the coatings was similar to that of their swelling ratios. CA, the coating that had the highest swelling ratio, released close to 90% of its PTX content in 5 hr, followed by the less wettable C and CP ($p < 0.05$) (Fig. 1(b)). The high swelling of CA allowed the PTX molecules in CA to diffuse more freely out of the polymer network following the concentration gradient.

In this test, 65–85% of PTX in the coatings was released within 5 hr of the test. *In vivo*, we expect PTX to be present in the local tissue hours after it is released, which could help reduce acute inflammation caused by neutrophils. When materials are implanted into the human body, inflammation takes place immediately. Neutrophils appear within minutes after an injury takes place and peak at 24 h to decontaminate the wound and prevent infection (Dovi, Szpaderska, & DiPietro, 2004). However, neutrophils have been shown to impair bone fracture healing (Chung, Cool, Scherer, Foster, & Xian, 2006; Grogaard, Gerdin, & Reikeras, 1990). Neutrophils are also believed to produce MCP-1 and IL-6 to attract macrophages. Macrophages recruit fibroblasts and cause fibrosis around implants (Hurst et al., 2001; Kasama, Strieter, Standiford, Burdick, & Kunkel, 1993). PTX have been shown to possibly prevent tissue damage by inhibiting neutrophil activities (Costantini et al., 2010; de Campos et al., 2008; Dovi et al., 2004; Weiss, Geor, Burris, & Smith, 1992). This reduced neutrophil activity can subsequently lead to a lesser degree of fibrosis which allows for better osseointegration at the implant/host tissue interface (Berman, 1989; Lin & Ciou, 2010).

3.4. Proliferation

All of the polymer coatings tested had significantly higher cell proliferation than Ti64 a week after seeding ($p < 0.01$) (Fig. 2). Higher osteoblast proliferation on chitosan and chitosan-based surfaces than on Ti and Ti64 surfaces has been previously reported (Bumgardner, Wiser, & Elder, et al., 2003; Lim, Wang, Shi, Poh, & Neoh, 2009; Shu, Ou, Wang, Zou, & Li, 2011). Higher cell proliferation on a chitosan coating than on a Ti surface has been attributed to the high density of positive charges on chitosan surfaces at physiological pH that attracted negatively-charged proteins and cells, despite that the fact that the Ti surface was more wettable (Bumgardner, Wiser, & Elder, et al., 2003). Alginate and pectin crosslinked chitosan materials have been reported to better promote bone cell growth because of their higher stiffness (Young's

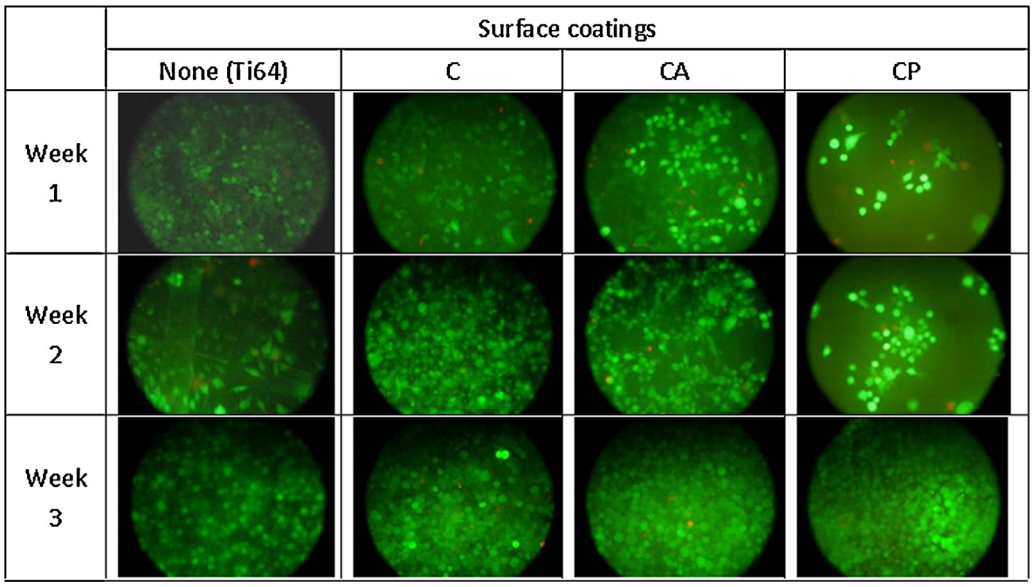

Fig. 3. Representative Live/Dead fluorescent stain images of cells on Ti64, C, CA, and CP over three weeks. Viable cells were stained green and dead cell stained red. Most of the cells observed on the different materials were viable.

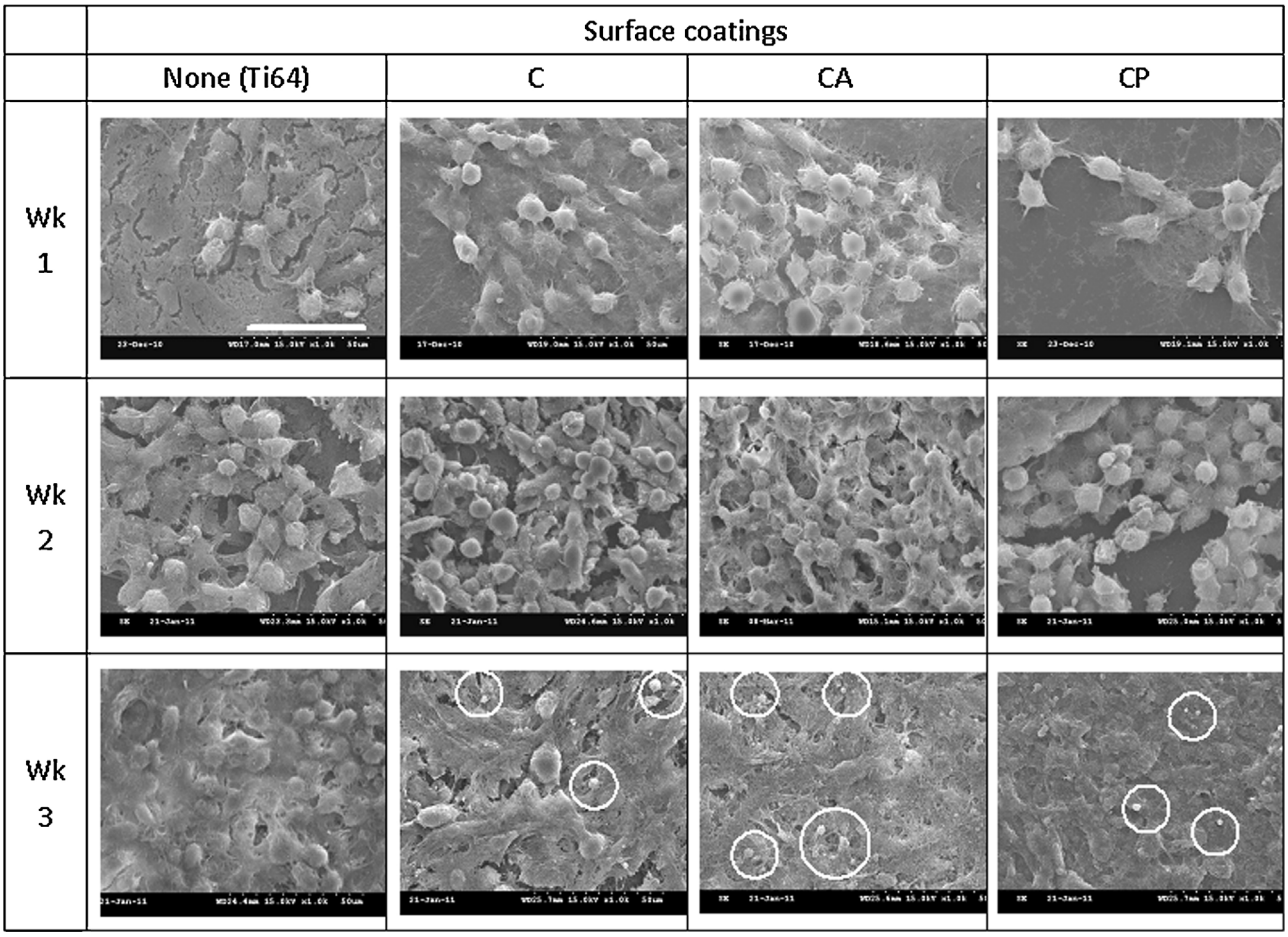

Fig. 4. Representative SEM micrographs of cells on Ti64, C, CA, and CP over three weeks. All micrographs are taken at same magnification (scale bar = 50 μm).

modulus), which was preferred by bone cells (Lin & Ciou, 2010; Lin & Yeh, 2010a).

By the end of the second and third weeks, all surfaces had similar levels of cell proliferation. The proliferation of cells from week 2 to week 3 was insignificant ($p > 0.05$). It is believed that the cells had reached confluency and stopped proliferating. It will later be shown in the results that these cells also started to express alkaline phosphatase and produce minerals.

3.5. Live/dead fluorescent stain

The photos from fluorescent staining showed that most of the cells were alive (green) after three weeks in the culture (Fig. 3). None of the surface materials appeared cytotoxic. Qualitatively speaking, cells displayed excellent viability on both the Ti64 and the polymer coatings. It's worth noting that the cells on CP grew in an uneven pattern. Before the cells on CP reached confluence, high densities of cells formed small lumps, and a few cells were observed around the peripheries of these lumps. As the culture time increased, the cells spread, and the lumps overlapped, forming cell layers. The reasons for this phenomenon were unclear to the authors. When chitosan was mixed with a pectin solution, cloudy lumps formed in the mixture. Therefore, it is speculated that when the pectin solution was placed on a chitosan coating, crosslinking did not take place homogeneously, and some spots were more favorable for cell attachment than others.

3.6. Cell morphology by scanning electron microscopy

The SEM micrographs of the cells growing on different surfaces for over three weeks are shown in Fig. 4. By the end of the first week, cells had attached to the surfaces and begun to proliferate. Filopodia of the cells could clearly be seen. Cells on C and CA had formed layers by the end of the first week while cells on CP formed aggregates. By the end of the second week, multiple layers of cells and extracellular matrix were observed on all surfaces. By week 3, most of the cells on C, CA, and CP were embedded in the abundant extracellular matrices they had secreted. In contrast, individual cells could be seen on Ti64. It appeared that cells on Ti64 had secreted less extracellular matrix, which was primarily made of type I collagen. This observation is supported by results shown in Fig. 5(b) that cells on Ti64 produced less type I collagen. Also, by week 3, mineralized nodules (circled in Fig. 4) were frequently observed on C, CA, CP, but not on Ti64. The extracellular matrix of the nodules predominantly consisted of type I collagen because calcium deposition is guided by collagen fibrils (Satomura, Hiraiwa, & Nagayama, 1991; Tong & Eppell, 2002). Naturally, because less collagen formed on Ti64, mineralized nodule formation was reduced.

3.7. Alkaline phosphatase (ALP) activity

The main functions of mature osteoblasts are to produce extracellular proteins (mainly type I collagen,) and to express ALP, which facilitates calcium phosphate formation. The ALP activity of cells on Ti64 remained at the same level over the 3-week period ($p > 0.05$). Considering the increase in the number of cells in weeks 2 and 3, the ALP activity per cell decreased during weeks 2 and 3 on Ti64. On the other hand, the ALP activity on the coatings increased significantly from week 1 to 2 as cells proliferated ($p < 0.05$) (Fig. 5(a)). While the number of cells on C, CA, and CP remained constant from week 2 to 3, the ALP activity on C decreased from week 2 to 3 while that of CA and CP remained unchanged. This indicated that cells on C stopped making ALP earlier than those on CA and CP. The difference in surface characteristics such as wettability and stiffness (which increases after crosslinking), alters cellular behavior (Subramanian & Lin, 2005).

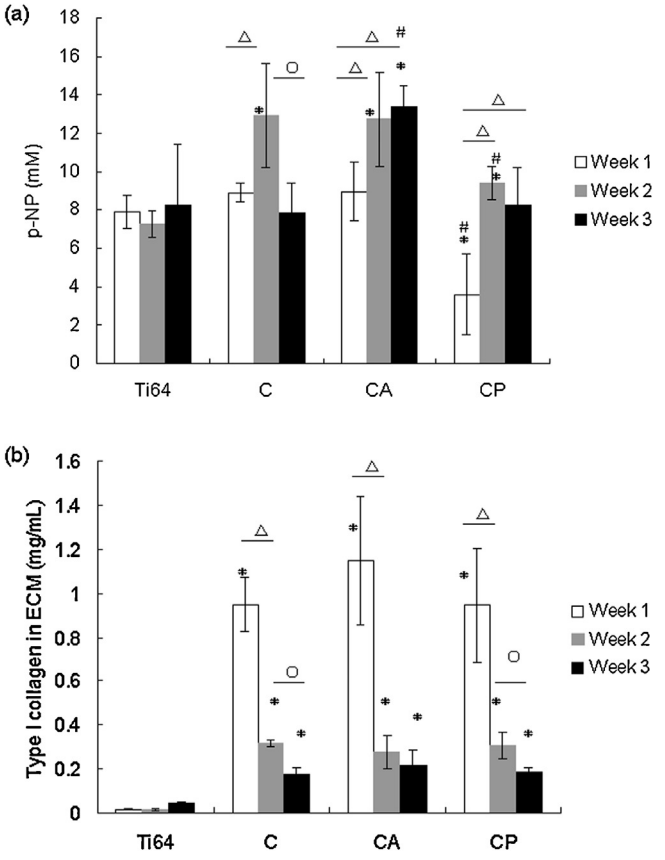

Fig. 5. (a) The alkaline phosphatase activity of cells measured by the amount of p-NP over three weeks and (b) the amount of type I collagen in the extracellular matrix of cells on Ti64, C, CA, and CP over three weeks. * and # indicate significant difference compared to Ti64 and C, respectively, measured at the same time ($p < 0.05$). △ and ○ indicate significant difference compared to week 1 and week 2, respectively, measured within the same material ($p < 0.05$).

Cells on CP showed lower ALP expression than those on C in weeks 1 and 2 ($p < 0.05$). We did not know the specific mechanisms but speculated that the uneven cell growth on CP had created different cell to cell interactions and thus different cellular activity.

Others have reported higher ALP activity in osteoblast cells on chitosan-based surfaces than on Ti and Ti alloy surfaces seven days after cell seeding (Lim et al., 2009; Shu et al., 2011). Cells associated with mineralized nodules exhibit high alkaline phosphatase activity (Satomura et al., 1991). As seen in Fig. 4, more nodules were present on the coatings where cells exhibited higher ALP activity than the Ti64 samples by week 3.

3.8. Expression of type I collagen and calcium deposition in the extracellular matrix

Compared to Ti64, C, CA, and CP had significantly more type I collagen in their extracellular matrices during the test ($p < 0.01$) (Fig. 5(b)). The amount of type I collagen on Ti64 stayed at base levels over the course of the three week testing period. Generally, less protein on a surface resulted in lower cell attachment and proliferation. However, the results in Fig. 2 did not show vast difference in cell proliferation between Ti64 and the coatings. The low quantity of extracellular collagen found on the Ti64 surface did not mean that the cells on the Ti64 surface did not actively produce type I collagen. The process of protein adsorption is a dynamic adsorption/desorption process which depends on factors such as hydrophobicity, surface charge, and pH (Andrade, Hlady, & Wei, 1992). As discussed in Section 3.4, there was higher density of

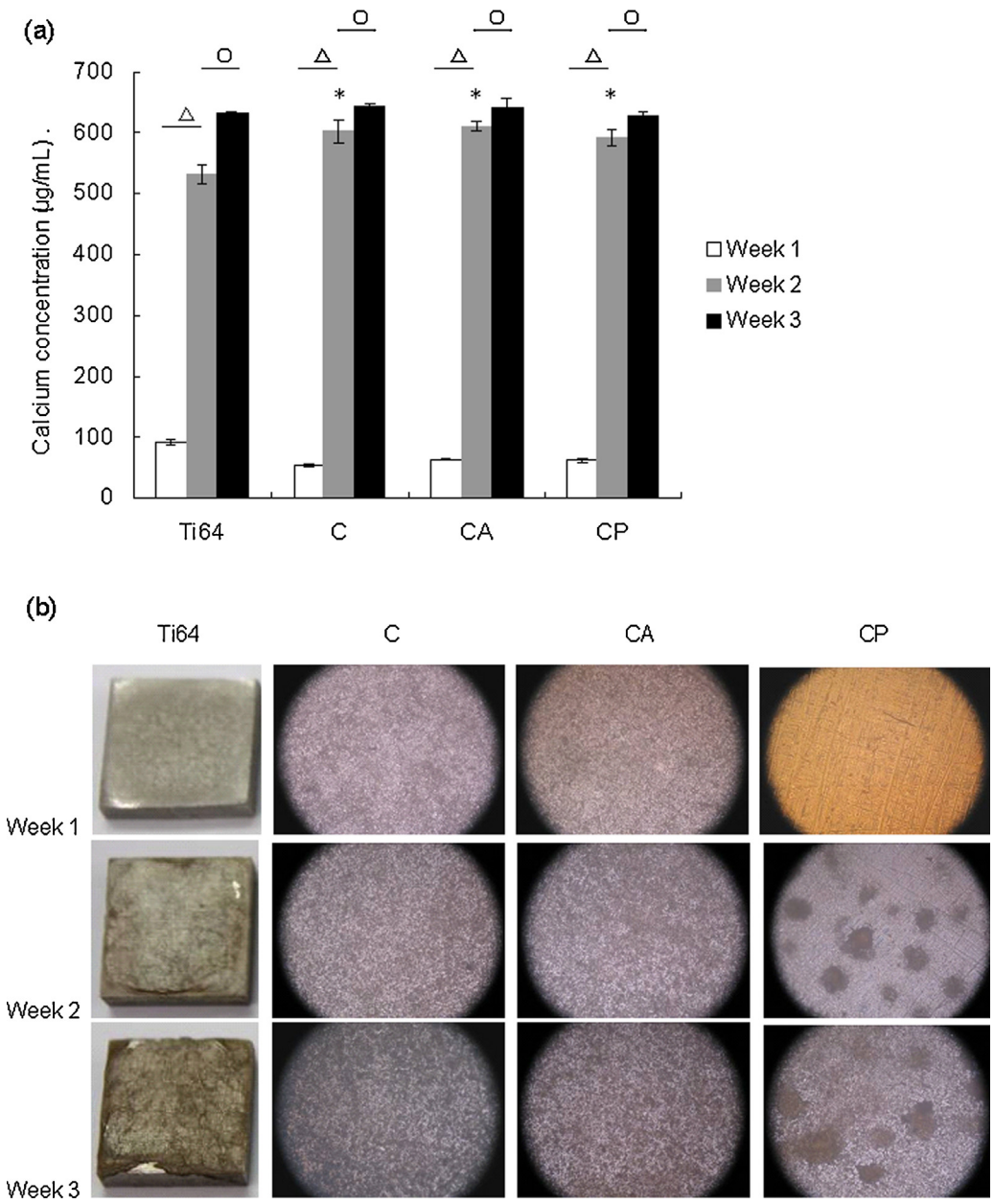

Fig. 6. (a) The amount of calcium in the extracellular matrix of cells on Ti64, C, CA, and CP over three weeks. * and # indicate significant difference compared to Ti64 and C, respectively, measured at the same time ($p < 0.05$). △ and ○ indicate significant difference compared to week 1 and week 2, respectively, measured within the same material ($p < 0.05$). (b) Representative pictures of a von Kossa stain of calcium on Ti64, C, CA, and CP over three weeks. The size of the Ti64 plate was 1 cm × 1 cm. The microscope magnification was 40×.

positive charge on chitosan than on Ti64 at physiological pH to attract negatively-charged proteins. Also, the surfaces of chitosan-based polymers were more hydrophobic (higher contact angle) than that of Ti64 and a general trend is that protein adsorption increases with increasing hydrophobicity of the surface (Nath, Hyun, Ma, & Chilkoti, 2004). It was expected that the combination of the above factors contributed to the higher type I collagen retention on the coatings than on bare Ti64 surface.

The amount of extracellular matrix collagen on C, CA, and CP decreased significantly from week 1 to week 2 ($p < 0.01$), and the decrease continued to week 3. Instead of making collagen, some osteoblast cells began to express ALP (Fig. 5(a)) and secrete calcium phosphate in weeks 2 and 3. The amount of type I collagen in the extracellular matrix then gradually decreased due to denaturation and desorption (Andrade, Hlady, & Wei, 1992; Leikina, Mertts, Kuznetsova, & Leikin, 2002). The extracellular matrices observed at week 3 (Fig. 4) should be mostly minerals and not collagen.

The secretion of calcium phosphate began at week 2 (Fig. 6(a)), corresponding to a significant increase in ALP activity by week 2 (Fig. 5(a)). This result meant that while the osteoblasts actively expressed ALP, the process of mineralization was greatly enhanced. The amount of calcium deposits continued to increase on all the surfaces from week 2 to 3 ($p < 0.05$) but the production of calcium seemed to slow down similar to that of cell proliferation (Fig. 2), possibly due to the limited space and possible cell apoptosis (Lian & Stein, 1995).

3.9. Von Kossa stain

For all samples, the color darkened each week (Fig. 6(b)), indicating the accumulation of calcium phosphate over time (Aubin,

Liu, Malaval, & Gupta, 1995; Clarke, 2008; Lian & Stein, 1995). Because there was an insignificant amount of matrix calcium measured (Fig. 6(a)), and, physiologically, osteoblasts were not likely to secrete calcium phosphate in the first week, the stains appearing in the first week were most likely from silver ions binding with free phosphate ions in the culture. A spotted staining pattern was observed on CP, corresponding to its uneven cell growth pattern (see Sections 3.5 and 3.6).

4. Conclusion

This was the first time that chitosan-based polymers were used to coat Ti-6Al-4V surfaces to study osteoblast cell behavior on the coatings. In addition to serving as a drug carrier, the coatings promoted faster cell proliferation, higher ALP expression, and greater collagen retention and calcium deposition. The crosslinking of alginate and pectin not only modified the drug release efficacy of chitosan, but also further enhanced its initial cell proliferation. CA even enhanced ALP expression for a longer period of time compared to C.

The *in vivo* bone healing process takes months. This research was limited in space and time for cell growth. Nonetheless, we believe that faster cell proliferation and the enhanced/prolonged ALP expression on CA coatings could reduce the degree of fibrosis and allow for the bone cells to have a longer window in which to produce calcium *in vivo*.

Acknowledgement

This work is sponsored by a grant from National Science Council (NSC 97-2221-E-027-001).

References

Abarrategi, A., Lopiz-Morales, Y., Ramos, V., Civantos, A., Lopez-Duran, L., Marco, F., et al. (2010). Chitosan scaffolds for osteochondral tissue regeneration. *Journal of Biomedical Materials Research Part A*, *95A*(4), 1132–1141.

Aksakal, B., & Hanyaloglu, C. (2008). Bioceramic dip-coating on Ti-6Al-4V and 316L SS implant materials. *Journal of Materials Science: Materials in Medicine*, *19*(5), 2097–2104.

Andrade, J., Hlady, V., & Wei, A. P. (1992). Adsorption of complex proteins at interfaces. *Pure and Applied Chemistry*, *64*(11), 1777–1781.

Aubin, J. E., Liu, F., Malaval, L., & Gupta, A. K. (1995). Osteoblast and chondroblast differentiation. *Bone*, *17*(Suppl. 2), 77S–83S.

Becker, D., Geissler, U., Hempel, U., Bierbaum, S., Scharnweber, D., Worch, H., et al. (2002). Proliferation and differentiation of rat calvarial osteoblasts on type I collagen-coated titanium alloy. *Journal of Biomedical Materials Research*, *59*(3), 516–527.

Berman, B. D. M. (1989). Pentoxifylline inhibits normal human dermal fibroblast in vitro proliferation, collagen, glycosaminoglycan, and fibronectin production, and increases collagenase activity. *Journal of Investigative Dermatology*, *92*, 605–610.

Bierbaum, S., Hempel, U., Geissler, U., Hanke, T., Scharnweber, D., Wenzel, K. W., et al. (2003). Modification of Ti6Al4V surfaces using collagen I, III, and fibronectin II. Influence on osteoblast responses. *Journal of Biomedical Materials Research Part A*, *67A*(2), 431–438.

Bumgardner, J. D., Wiser, R., Elder, S. H., Jouett, R., Yang, Y., & Ong, J. L. (2003). Contact angle, protein adsorption and osteoblast precursor cell attachment to chitosan coatings bonded to titanium. *Journal of Biomaterials Science-Polymer Edition*, *14*(12), 1401–1409.

Bumgardner, J. D., Wiser, R., Gerard, P. D., Bergin, P., Chestnutt, B., Marini, M., et al. (2003). Chitosan: potential use as a bioactive coating for orthopaedic and craniofacial/dental implants. *Journal of Biomaterials Science-Polymer Edition*, *14*(5), 423–438.

Chung, R., Cool, J. C., Scherer, M. A., Foster, B. K., & Xian, C. J. (2006). Roles of neutrophil-mediated inflammatory response in the bony repair of injured growth plate cartilage in young rats. *Journal of Leukocyte Biology*, *80*(6), 1272–1280.

Clarke, B. (2008). Normal bone anatomy and physiology. *Clinical Journal of the American Society of Nephrology*, *3*(Suppl. 3), S131–S139.

Cleries, L., Fernandez-Pradas, J. M., & Morenza, J. L. (2000). Bone growth on and resorption of calcium phosphate coatings obtained by pulsed laser deposition. *Journal of Biomedical Materials Research*, *49*(1), 43–52.

Costantini, T. W., Deree, J., Peterson, C. Y., Putnam, J. G., Woon, T., Loomis, W. H., et al. (2010). Pentoxifylline modulates p47phox activation and downregulates neutrophil oxidative burst through PKA-dependent and -independent mechanisms. *Immunopharmacology and Immunotoxicology*, *32*(1), 82–91.

de Campos, T., Deree, J., Martins, J. O., Loomis, W. H., Shenvi, E., Putnam, J. G., et al. (2008). Pentoxifylline attenuates pulmonary inflammation and neutrophil activation in experimental acute pancreatitis. *Pancreas*, *37*(1), 42–49.

Dovi, J. V., Szpaderska, A. M., & DiPietro, L. A. (2004). Neutrophil function in the healing wound: Adding insult to injury? *Thrombosis and Haemostasis*, *92*(2), 275–280.

Geissler, U., Hempel, U., Wolf, C., Scharnweber, D., Worch, H., & Wenzel, K. (2000). Collagen type I-coating of Ti6Al4V promotes adhesion of osteoblasts. *Journal of Biomedical Materials Research*, *51*(4), 752–760.

Greene, A. H., Bumgardner, J. D., Yang, Y., Moseley, J., & Haggard, W. O. (2008). Chitosan-coated stainless steel screws for fixation in contaminated fractures. *Clinical Orthopaedics and Related Research*, *466*(7), 1699–1704.

Grogaard, B., Gerdin, B., & Reikeras, O. (1990). The polymorphonuclear leukocyte: Has it a role in fracture healing? *Archives of Orthopaedic and Trauma Surgery*, *109*(5), 268–271.

Head, W. C., Bauk, D. J., & Emerson, R. H., Jr. (1995). Titanium as the material of choice for cementless femoral components in total hip arthroplasty. *Clinical Orthopaedics and Related Research*, *311*, 85–90.

Hurst, S. M., Wilkinson, T. S., McLoughlin, R. M., Jones, S., Horiuchi, S., Yamamoto, N., et al. (2001). Il-6 and its soluble receptor orchestrate a temporal switch in the pattern of leukocyte recruitment seen during acute inflammation. *Immunity*, *14*(6), 705–714.

Kasama, T., Strieter, R. M., Standiford, T. J., Burdick, M. D., & Kunkel, S. L. (1993). Expression and regulation of human neutrophil-derived macrophage inflammatory protein 1 alpha. *Journal of Experimental Medicine*, *178*(1), 63–72.

Kim, T. H., Park, Y. H., Kim, K. J., & Cho, C. S. (2003). Release of albumin from chitosan-coated pectin beads in vitro. *International Journal of Pharmaceutics*, *250*(2), 371–383.

Klock, G., Pfeffermann, A., Ryser, C., Grohn, P., Kuttler, B., Hahn, H. J., et al. (1997). Biocompatibility of mannuronic acid-rich alginates. *Biomaterials*, *18*(10), 707–713.

Kokkonen, H., Cassinelli, C., Verhoef, R., Morra, M., Schols, H. A., & Tuukkanen, J. (2008). Differentiation of osteoblasts on pectin-coated titanium. *Biomacromolecules*, *9*(9), 2369–2376.

Kokkonen, H., Niiranen, H., Schols, H. A., Morra, M., Stenback, F., & Tuukkanen, J. (2010). Pectin-coated titanium implants are well-tolerated in vivo. *Journal of Biomedical Materials Research Part A*, *93*(4), 1404–1409.

Kokkonen, H., Verhoef, R., Kauppinen, K., Muhonen, V., Jorgensen, B., Damager, I., et al. (2012). Affecting osteoblastic responses with in vivo engineered potato pectin fragments. *Journal of Biomedical Materials Research Part A*, *100*(1), 111–119.

Leikina, E., Mertts, M. V., Kuznetsova, N., & Leikin, S. (2002). Type I collagen is thermally unstable at body temperature. *Proceedings of the National Academy of Sciences USA*, *99*(3), 1314–1318.

Li, J. J., Sun, H., Sun, D., Yao, Y. L., Yao, F. L., & Yao, K. D. (2011). Biomimetic multicomponent polysaccharide/nano-hydroxyapatite composites for bone tissue engineering. *Carbohydrate Polymers*, *85*(4), 885–894.

Lian, J. B., & Stein, G. S. (1995). Development of the osteoblast phenotype: molecular mechanisms mediating osteoblast growth and differentiation. *The Iowa Orthopaedic Journal*, *15*, 118–140.

Lim, T. Y., Wang, W., Shi, Z., Poh, C. K., & Neoh, K. G. (2009). Human bone marrow-derived mesenchymal stem cells and osteoblast differentiation on titanium with surface-grafted chitosan and immobilized bone morphogenetic protein-2. *Journal of Materials Science: Materials in Medicine*, *20*(1), 1–10.

Lin, H. Y., & Ciou, S. Y. (2010). Modifications of alginate-based scaffolds and characterizations of their pentoxifylline release properties. *Carbohydrate Polymers*, *80*(2), 574–580.

Lin, H. Y., & Yeh, C. T. (2010a). Alginate-crosslinked chitosan scaffolds as pentoxifylline delivery carriers. *Journal of Materials Science: Materials in Medicine*, *21*(5), 1611–1620.

Lin, H. Y., & Yeh, C. T. (2010b). Controlled release of pentoxifylline from porous chitosan–pectin scaffolds. *Drug Delivery*, *17*(5), 313–321.

Nath, N., Hyun, J., Ma, H., & Chilkoti, A. (2004). Surface engineering strategies for control of protein and cell interactions. *Surface Science*, *570*(1/2), 98–110.

Park, J. W., Kim, H. K., Kim, Y. J., Jang, J. H., Song, H., & Hanawa, T. (2010). Osteoblast response and osseointegration of a Ti-6Al-4V alloy implant incorporating strontium. *Acta Biomaterialia*, *6*(7), 2843–2851.

Satomura, K., Hiraiwa, K., & Nagayama, M. (1991). Mineralized nodule formation in rat bone marrow stromal cell culture without beta-glycerophosphate. *Bone and Mineral*, *14*(1), 41–54.

Schwartz, Z., Griffon, D. J., Fredericks, L. P., Lee, H. B., & Weng, H. Y. (2011). Hyaluronic acid and chondrogenesis of murine bone marrow mesenchymal stem cells in chitosan sponges. *American Journal of Veterinary Research*, *72*(1), 42–50.

Shu, Y., Ou, G. M., Wang, L., Zou, J. C., & Li, Q. L. (2011). Surface modification of titanium with heparin-chitosan multilayers via layer-by-layer self-assembly technique. *Journal of Nanomaterials*, vol. 2011 (*2011*), article ID 423686.

Singhatanadgit, W. (2009). Biological responses to new advanced surface modifications of endosseous medical implants. *Bone and Tissue Regeneration Insights*, *2*, 1–11.

Subramanian, A., & Lin, H. Y. (2005). Crosslinked chitosan: Its physical properties and the effects of matrix stiffness on chondrocyte cell morphology and proliferation. *Journal of Biomedical Materials Research Part A*, *75A*(3), 742–753.

Tang, M., Chen, W., Weir, M. D., Thein-Han, W., & Xu, H. H. (2012). Human embryonic stem cell encapsulation in alginate microbeads in macroporous

calcium phosphate cement for bone tissue engineering. *Acta Biomaterialia*, *8*(9), 3436–3445.

Tong, W. D., & Eppell, S. J. (2002). Control of surface mineralization using collagen fibrils. *Journal of Biomedical Materials Research*, *61*(3), 346–353.

Weiss, D. J., Geor, R. J., Burris, S. M., & Smith, C. M., 2nd. (1992). Effects of pentoxifylline on equine neutrophil function and flow properties. *Canadian Journal of Veterinary Research*, *56*(4), 313–317.

Xing, J., Hou, T., Luobu, B., Luo, F., Chen, Q., Li, Z., et al. (2013). Anti-infection tissue engineering construct treating osteomyelitis in rabbit tibia. *Tissue Engineering Part A*, *19*(1-2), 255–263.

Yang, C., Frei, H., Rossi, F. M., & Burt, H. M. (2009). The differential in vitro and in vivo responses of bone marrow stromal cells on novel porous gelatin-alginate scaffolds. *Journal of Tissue Engineering and Regenerative Medicine*, *3*(8), 601–614.